Research Article

Design of a D-Q Axis Controlled Micro Inverter with Flyback Converter for Grid-Connected PV Systems

Elif Baldan, Ozgur Celik, Hüseyin Eristi

***Abstract*—Inverters are one of the most important components of photovoltaic (PV) systems. Inverters are utilized as an operational interface between PV panels and the power grid or residential applications. In order to provide high system efficiency and reliable power transfer from PV panels, intensive studies have been conducted on the power circuit topologies and control structures of these inverters. In this paper, a two-stage grid-connected microinverter is designed. There is a flyback converter on the DC-DC side and a full-bridge inverter structure on the DC-AC side. The designed microinverter has the ability to amplify the input voltage. The DC voltage amplified at the inverter output is converted at the output of the microinverter to be suitable for the grid. The flyback converter is controlled by a maximum power point tracking (MPPT) algorithm and a PI controller. On the other side, the full-bridge inverter section is controlled by a D-Q axis controller. The system response is analyzed under different irradiance values. The control structures created in the designed microinverter accurately tracked the maximum power point, and maximum power transfer to the grid is observed according to different irradiance values.**

***Index Terms*—Photovoltaic panel, maximum power point tracking, flyback converter, microinverter, D-Q axis control**

I. INTRODUCTION

Population growth and developments in technology and industry constantly increase the need for energy. Fossil fuel resources are limited, and efficient energy production cannot be achieved due to the negative factors that occur after using fossil fuels. For this reason, the search for new energy to reduce the negative effects of global warming, environmental pollution, and carbon emissions has started [1]. Renewable energy sources are attracting great interest due to their sustainability, widespread availability, and nature-friendliness. Compared to other renewable energy sources, solar energy makes it possible to use photovoltaic (PV) panels in almost any area by suitably placing them, thanks to their different arrays [2]. PV systems, which have seen a remarkable increase in recent years, are of two types: off-grid and on-grid systems. In off-grid systems, a storage element such as a battery is used. There is no need for this in on-grid systems. This is because the electricity grid already acts as a storage area. PV systems are used in combination with DC-DC converters and DC-AC inverter circuits based on various power electronics systems for direct transmission to the grid [3], [4]. There are different inverter structures for grid-connected systems according to their power capacities. Centralized inverters are used in high-power systems. In such systems, PV panels are connected in series to form an array. These arrays are also connected in parallel, and high powers are obtained. However, failure or partial shading affects the efficiency. String inverters are used at lower powers than central inverters. String inverters are added at the end of the arrays created by connecting the panels in series. The string inverter is connected to each string separately [5]. However, the efficiency problem of partial shading in central inverters is also encountered in string inverters [6]. The microinverter, which is used in small power, is an inverter type that has become very popular in recent years among inverter types [3].

The microinverter has the advantages of being suitable for use in rooftop applications, being able to connect to each panel separately thanks to its plug-and-play feature, and reducing the size of DC cables. Since the microinverter has a panel-specific maximum power point tracking (MPPT) feature, it can overcome partial shading conditions. Since panel-specific control is possible, system efficiency is protected. Microinverters can be implemented using single-stage or two-stage power conversion topologies. In a two-stage configuration, a DC-DC converter regulates an input voltage, followed by a DC-AC inverter stage responsible for grid-adaptive power output. [4], [7]. DC-DC converters are generally classified into three main types according to the desired application: buck (step-down), boost (step-up), and buck-boost converters. Among these converters, the flyback converter model has many advantages. Flyback converters are extensively utilized in power electronics owing to their suitability for high-frequency operation, ease of amplifying the input voltage, and simple topology. The flyback converter amplifies the voltage generated from the panel with the

Elif Baldan, is with the Department of Electrical and Electronics Engineering, Faculty of Engineering, Mersin University, Mersin, Turkiye, (Email: ebaldan@mersin.edu.tr). https://orcid.org/0009-0007-1248-4064

Özgür Çelik, is with the Department of Energy Systems Engineering, Adana Alparslan Turkes Science and Technology University Adana, Turkiye, (Email: ozgurcelik@atu.edu.tr). https://orcid.org/0000-0002-7683-2415

Hüseyin Erişti, is with the Department of Electrical and Electronics Engineering, Faculty of Engineering, Mersin University, Mersin, Turkiye, (Email: heristi@mersin.edu.tr). https://orcid.org/0000-0003-1474-9170

Manuscript received Jun 30, 2025; accepted Aug 25, 2025.
DOI: 10.17694/bajece.1730786

required control algorithms. Many algorithms have been developed for converter control. The main objective is to maximize the power transfer from the PV panel to the grid. For this purpose, Maximum Power Point Tracking (MPPT) algorithms are used to continuously operate the PV system at the optimal power point. [8]. The second stage of microinverter design involves the DC-AC inverter, which converts the boosted DC voltage into an alternating AC voltage suitable for grid integration. The output is filtered through an LCL filter and transferred to the grid. Full-bridge inverters are designed to increase overall efficiency [9], [10]. Many control systems have also been designed for the DC-AC inverter controller [11]–[13]. A flyback microinverter with an analog divider is designed to send current to the grid and achieve a high power factor. Both high efficiency and stable MPPT control are observed [14]. The energy harvesting efficiency of the MPPT algorithm applied in a 250W system is measured as 99% in a study conducted in MATLAB/Simulink. In this way, it is observed that it transfers high-quality power to the grid [15]. In one of the studies, based on the advantage of the low number of components of the flyback structure, a DC-DC flyback structure with multiple parallel switching is constructed [16]. In another study, the state space average method is used for the flyback converter having an isolated structure, and the analyses are performed in MATLAB/Simulink [17]. In another study, in the design of a flyback-based microinverter, the perturb and observe (P&O) algorithm is used as the MPPT algorithm [18]. In another study on power tracking efficiency under different irradiances, convergence and performance analyses are performed using the MPPT algorithm [19]. A comparison of the flyback-based microinverter with other inverters in terms of power harvesting under partial shading conditions is made, and its advantages are emphasized. It is observed that it produces more power than other inverters [20]. In another study on the stability of power conversion, a microinverter with an MPPT-controlled interleaved flyback converter structure is designed [21]. In grid-connected systems, control strategies based on the D-Q reference frame are frequently employed [6]. Experimental and simulation results indicate significant improvements in system behavior and overall performance [22].

In this paper, a flyback converter-based grid-connected two-stage microinverter is designed. The flyback converter side is controlled by a PI controller to ensure operation at the maximum power point. The reference operating point for the flyback converter is provided by an MPPT algorithm. In the inverter section, a voltage control structure is designed in addition to the D-Q-oriented current controller. Apart from the aforementioned studies on the design of the microinverter, this paper includes the design of the microinverter with a flyback converter and investigates the two-stage structure control separately.

The remainder of this paper is organised as follows. The general schematic of the designed microinverter is described in Section 2. The details of the flyback converter and the control algorithm are described in Section 3. Inverter design, which is the second stage of the microinverter, and the related control blocks are given in Section 4. Section 5 covers the LCL filter design between the grid and the inverter. The designed microinverter and simulation results are given in Section 6. Finally, Section 7 summarizes and concludes the proposal.

II. Circuit Configuration Of The Designed Microinverter

The schematic representation of the designed microinverter circuit, comprising a flyback converter, a full-bridge inverter, and an LCL filter, is illustrated in Figure 1. The flyback converter is located between the PV panel and the inverter. It consists of a high-frequency transformer, a MOSFET, a diode, and a capacitor. The duty cycle of the flyback converter is regulated through a combination of the P&O algorithm and a PI controller. The transformer of the flyback converter has a conversion ratio of 1:8. The voltage of the PV panel is stepped up to 380 V by the flyback converter. This boosted voltage value provides the input voltage of the DC-AC inverter. The single-phase full-bridge inverter consists of four MOSFET switches and is controlled via a voltage controller in conjunction with a D-Q axis current controller to facilitate grid current injection. The LCL filter is used to obtain a sine wave at the output of the microinverter by reducing harmonics. Table I summarizes the key electrical specifications of the PV panel utilized in this study. In the following sections, the flyback converter, full bridge rectifier inverter, and the required control structures are presented in detail.

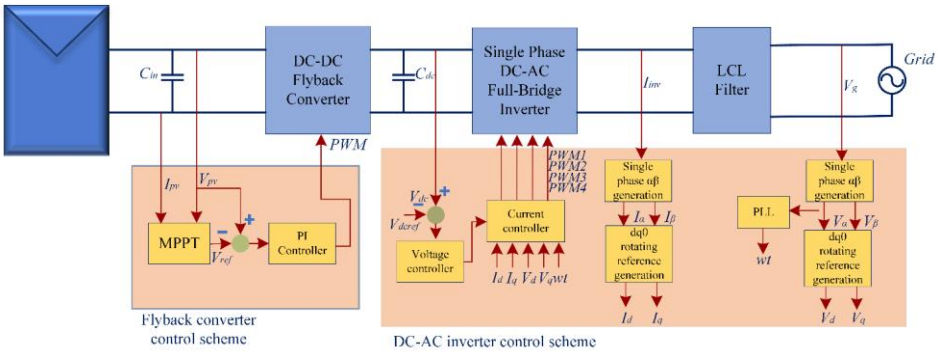

Fig. 1. Grid-connected microinverter circuit basic schematic and control blocks

TABLE I
CHARACTERISTIC FEATURES OF PV PANELS

Parameter	Symbol	Value
Maximum Power	P_{MPP}	269.919 W
Maximum Power Voltage	V_{MPP}	35.1 V
Maximum Power Current	I_{MPP}	7.69 A
Open Circuit Voltage	V_{OC}	44.5 V
Short Circuit Current	I_{SC}	8.42 A
Temperature coefficient of current	K_i	0.084299(%/deg.C)
Temperature coefficient of voltage	K_v	-0.3631 (%/deg.C)
Number of serial cells	N_s	72

III. FLYBACK CONVERTER

The flyback converter topology has an isolated topology. This topology is a modified version of the buck-boost converter. An isolated transformer is used in place of the coil used for the inductor. Owing to the transformer used, the voltage gain is higher than other converters. This converter is very prominent in microinverter applications in PV systems due to its features such as reduced component count, support for MPPT operation, wide power range, and increased input voltage. [5]. The operating principle of the flyback converter is fundamentally derived from the buck-boost converter topology. A typical flyback converter circuit diagram is depicted in Figure 2.

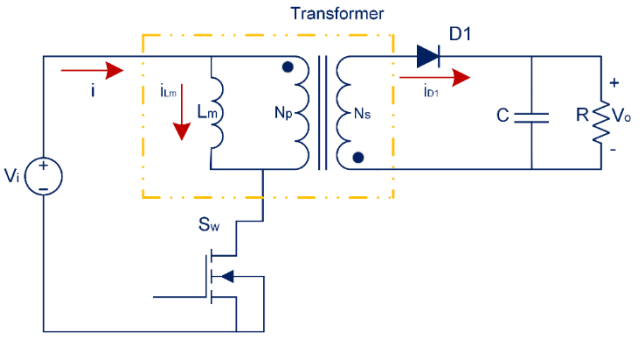

Fig. 2. Main circuit of a flyback converter

The mathematical relationship governing the input and output voltages in the above circuit is given below;

$$\frac{V_o}{V_i} = n\frac{D}{(1-D)} \quad (1)$$

In this context, V_i and V_o correspond to the converter's input and output voltages, respectively. The symbol n indicates the turns ratio of the transformer, while D represents the converter's duty cycle. The following equation defines the minimum allowable value of magnetizing inductance at the transformer's primary winding;

$$L_m = \frac{n^2 V_o\,(1-D_{min})^2}{2 f_s I_{omin}} \quad (2)$$

where f_s refers to the switching frequency, and I_o indicates the output current. According to the oscillations in the output voltage, the output filter capacitor is expressed as;

$$C_{min} = \frac{V_o\, D_{max}}{f_s R_{min} \Delta V_o} \quad (3)$$

where ΔV_o denotes the maximum acceptable peak-to-peak ripple of the output voltage, while R_{min} refers to the minimum load resistance. In a flyback converter design, the switching period consists of three different intervals. During certain intervals, the load is supplied solely by the output capacitor. The magnetizing current decreases to zero, indicating operation in discontinuous conduction mode (DCM).

- Stage 1 (t_0>t>t_1)

When the control signal turns on the MOSFET, the magnetizing inductance current begins to rise as a result of the applied input voltage V_g. During this phase, the switch conducts the magnetizing current, and this state is maintained until the control signal turns the MOSFET off.

$$i_{Q1} = i_{Lm} = \frac{V_g}{L_m} t \quad (4)$$

- Stage 2 (t_1>t>t_2)

In this stage i_{Q1} = 0 and $i_{D1} = I_{D1\_max}$. The switch closes, and the diode $D1$ opens. The energy stored in the magnetizing inductance is released through the secondary winding of the transformer and delivered to the output load.

$$i_{D1} = I_{D1\_max} - \frac{V}{L_s} t \quad (5)$$

$$I_{D1\_max} = I_{LM\_max} n \quad (6)$$

L_s is the secondary winding in the transformer, and I_{D1_max} is the maximum current through the diode. This phase ends when the diode current reaches zero.

- Stage 3 (t_2>t>t_3)

The energy of the magnetizing inductance is reset at this stage. The interval begins with the cessation of the diode current and concludes when the gate control signal is reapplied to the switch $Q1$ [23].

A. Perturb and Observe (P&O) Algorithm

Implementing an MPPT algorithm is essential for maximizing the power extracted from a photovoltaic (PV) panel under dynamic environmental conditions, including fluctuations in irradiance and temperature [24]. Among MPPT algorithms, the P&O algorithm is mainly utilized owing to its straightforward implementation and reliable performance. The duty cycle is determined according to the current and voltage values measured from the PV panel to reach the maximum power point [25]. The flowchart of the algorithm is given in Figure 3. The duty cycle is determined by calculating the values of ΔP_{pv} and ΔV_{pv}. In this article, a V_{ref} value is obtained from the output of the P&O algorithm for the flyback converter. This value is compared with the voltage from the PV panel and passed through a PI controller. The MOSFET in the flyback converter is then switched with the PWM signal obtained by performing the necessary operations. Figure 1 shows the control scheme of the flyback converter.

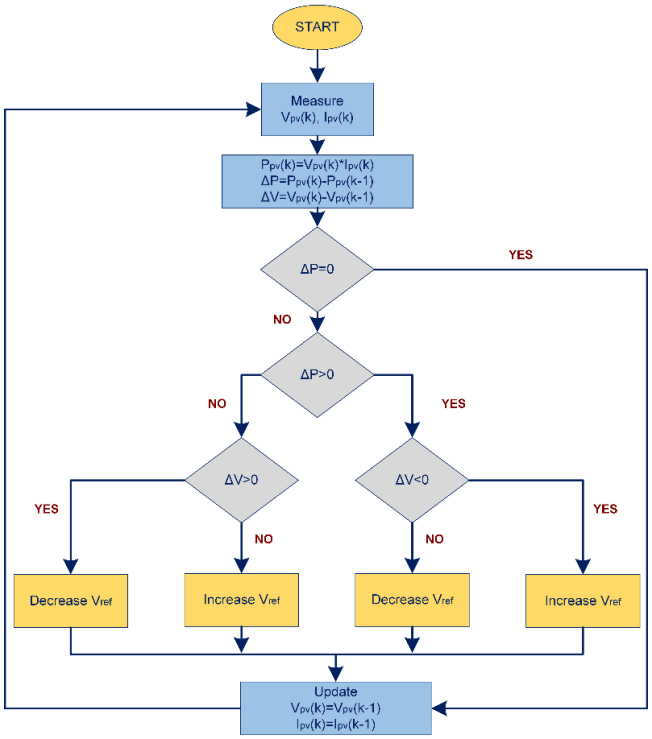

Fig. 3. Flowchart of the perturb and observe algorithm

IV. DC-AC Inverter Design And Control Topology

A. DC-AC Inverter Design

To convert DC voltage to AC voltage, a conventional single-phase full-bridge inverter structure is used. There are four MOSFETs in the circuit topology of the inverter. Looking at the circuit given in the figure, S1 and S4 MOSFETs are in conduction at the same time. When S1 and S4 MOSFETs are in conduction, S2 and S3 MOSFETs will be in the cutoff. The same is true for the reverse. In this way, the DC voltage supplied by the flyback converter is subsequently converted into an AC voltage by the inverter stage. Figure 4 shows the grid-connected full-bridge inverter circuit.

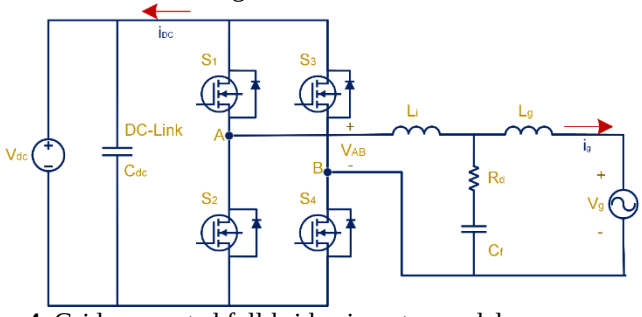

Fig. 4. Grid-connected full-bridge inverter model

- When S1 and S4 are conducting $V_{AB} = V_{DC}$
- When S2 and S3 are conducting $V_{AB} = -V_{DC}$

B. Control Topology of the Inverter

A control structure is required for the PWMs of the MOSFETs in the inverter circuit. To transfer the current to the grid, the necessary control structures are created. Firstly, Park-Clarke transformations of inverter current and grid voltage expressions in sine form are made. D-Q axis expressions need to be obtained. But first, the α-β (Clarke) transformation must be done. Clarke transformations are performed in three-phase systems. Clarke transformations cannot be performed in single-phase systems. Therefore, the orthogonal wave generation method is used to obtain the expression in the α-β axis. The sinusoidal signal is shifted by 90 degrees. In this way, expressions are generated in the α-β axis [8]. Phase position information is obtained with the PLL block and V_d and V_q expressions are obtained using the generated V_α and V_β expressions. The same process is done by taking the inverter's current information. Using the phase position information and the generated I_α and I_β expressions, I_d and I_q expressions are generated. After the D-Q axis is passed, the current controller process is started. Here, I_{dref} and I_{qref} values are determined. I_{qref} value is taken as zero since reactive power and phase shift are not desired. I_{dref} value expresses the current value desired to be transferred to the grid. This value is determined by a voltage controller. The voltage value on the DC link capacitor at the inverter input is compared with the DC link reference voltage. Then, the I_{dref} value is obtained by passing it through a PI controller. At the output of the current controller, the obtained expressions are subjected to the necessary operations, inverse Park-Clarke transformed, and converted to sinusoidal form. As a final process, the obtained expression is divided by the DC link reference voltage, and PWM signals are generated. In this way, the MOSFETs in the inverter structure are switched.

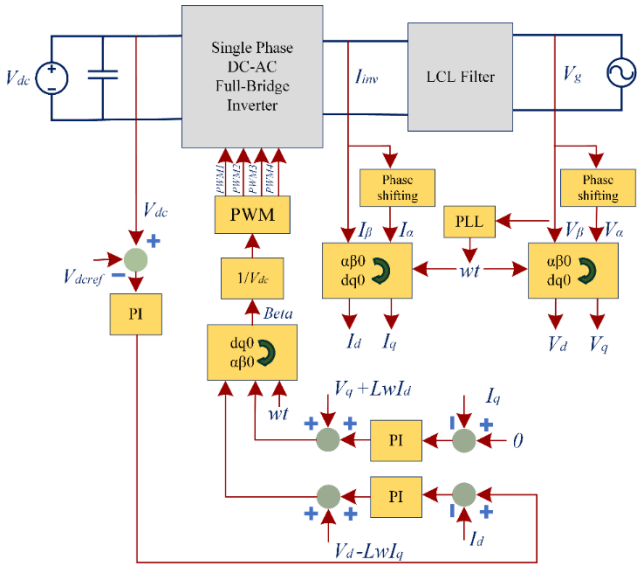

Fig. 5. D-Q axis current-controlled grid-connected inverter control scheme

V. LCL Filter Design

An LCL filter is employed to attenuate the output current ripple of the microinverter. It is capable of effectively suppressing high-frequency harmonics even with relatively

small inductance values. A critical design parameter for the LCL filter is its cut-off frequency, which should be set to approximately half of the minimum switching frequency. However, due to its resonant characteristics, the LCL filter is susceptible to oscillations and tends to amplify frequency components near the cut-off point. Therefore, a damping resistor is added to the filter [26]. Reactive power requirements can lead to resonance of the capacitor with grid interaction. Therefore, a series resistor is added to the capacitor for active and passive damping. The equations necessary for LCL filter design are given in the following order.

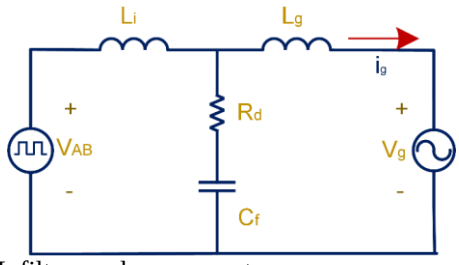

Fig. 6. LCL filters and components

$$Z_b = \frac{U_n^2}{P_n} \quad (7)$$

where U_n is the peak-to-peak inverter output RMS voltage. P_n refers to the nominal active power,

$$C_b = \frac{1}{2\pi f_g Z_b} = \frac{1}{w_g Z_b} \quad (8)$$

where f_g is the grid frequency.

First, the inverter-side inductor (L_i) is designed to limit the output current ripple to 10% of the nominal value.

$$L_i = \frac{V_{DC}}{16 f_s \Delta I_{Lmax}} \quad (9)$$

where V_{DC} is the DC voltage value.

$$\Delta I_{Lmax} = 0.01 \frac{P_n \sqrt{2}}{U_n} \quad (10)$$

The value of the filter capacitor is calculated as the product of 5% of the maximum grid-compliant power factor and the base capacitance of the system.

$$C_f = 0.05 C_b \quad (11)$$

The inductor value of the grid side (L_g) is calculated as follows.

$$L_g = r L_i \quad (12)$$

The final step in the filter design process involves determining the resonant frequency. Resonant frequency is an important factor affecting system behavior in real-time applications. In grid-connected systems, undesired resonance effects can cause instability or harmonic amplification, especially in weak grid conditions or when multiple inverters are involved. This frequency should be distant from the grid frequency and set to at least half of the converter's switching frequency. The resonant frequency is evaluated as

$$f_{res} = \frac{1}{2\pi} \sqrt{\frac{L_i + L_g}{L_i L_g C_f}} \quad (13)$$

The oscillations and unsteady states of the filter are reduced by a series resistor connected to the capacitor. This is called passive analysis. The damping resistance is given as [27].

$$R_d = \frac{1}{3(2\pi f_{res}) C_f} = \frac{1}{3 w_{res} C_f} \quad (14)$$

The parameters required for the filter design are given in Table II.

TABLE II
MICROINVERTER DESIGN VALUES

Parameter	Symbol	Value
Output voltage	V_{DC}	380 V
Magnetizing inductance	L_m	6.3 µH
Output capacitor	C	1000 µF
Turn ratio	n	1:8
Grid voltage	V_g	220 V_{RMS}
Inverter side inductor	L_i	11.8 mH
Inductance of the grid side filter	L_g	5.9 mH
Filter capacitor	C_f	1 µF
Switching frequency for the flyback converter	f_{s_conv}	100 kHz
Switching frequency for the inverter	f_{s_inv}	20 kHz
Grid frequency	f_g	50 Hz
Damping resistance	R_d	21 Ω

VI. SIMULATION RESULTS AND DISCUSSIONS

The microinverter design is performed in MATLAB/Simulink. The system components are a PV module, a flyback converter, a DC link capacitor, a full bridge inverter, and an LCL filter. This study aims to assess the stable grid power injection capability of the designed microinverter and the effectiveness of its MPPT operation. Figure 7 illustrates the irradiance applied to the PV panel at different values while maintaining a constant panel temperature. The irradiation starts with 1000 W/m^2. After one second, the irradiance value decreases to 500 W/m^2. Then, the irradiance value increases to 800 W/m^2 at 2.5 seconds

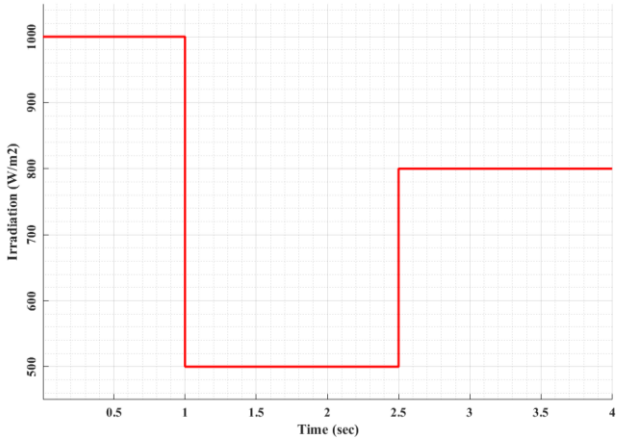

Fig. 7. The irradiation of the PV panel

The voltage corresponding to the maximum power point of the PV panel is 35 V. The graph presented in Figure 8 indicates that, at an irradiance level of 1000 W/m², the maximum power point occurs at approximately 35 V. In Figure 9, the DC link voltage also reaches 380 V output after about 0.4 seconds. After the 1st second, the irradiance value decreases. After the irradiance value decreases to 500 W/m², the current injected into the grid decreases. However, it is observed that the DC link voltage decreases until the grid current decreases and reaches a suitable value. The DC link could not be fed sufficiently until the grid current reaches the appropriate point. At this moment, I_{dref} reference current value is reduced by the voltage controller. The DC bus voltage starts to increase to 380 V again. The grid current reaches the optimum value with the current controller created with the D-Q control structure. After the grid current reaches the correct value, the DC bus voltage reaches 380 V. At 2.5 seconds, the irradiance value is increased again. Figure 10 illustrates the grid voltage. In Figure 11, the variation of the current injected into the grid is presented in zoomed graphs. In this case, the DC bus is overfed until the grid current rises to the required value. The voltage controller subsequently establishes the reference current value, which is regulated by the current controller to maintain grid current stability. Following this control process, the DC bus voltage stabilizes at 380 V.

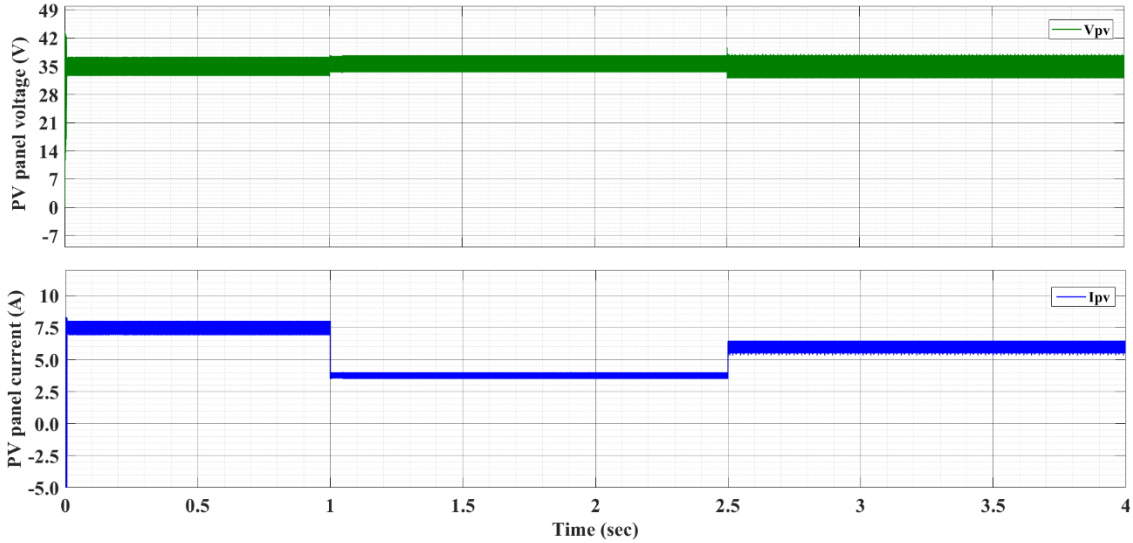

Fig. 8. The voltage and current of the PV panel

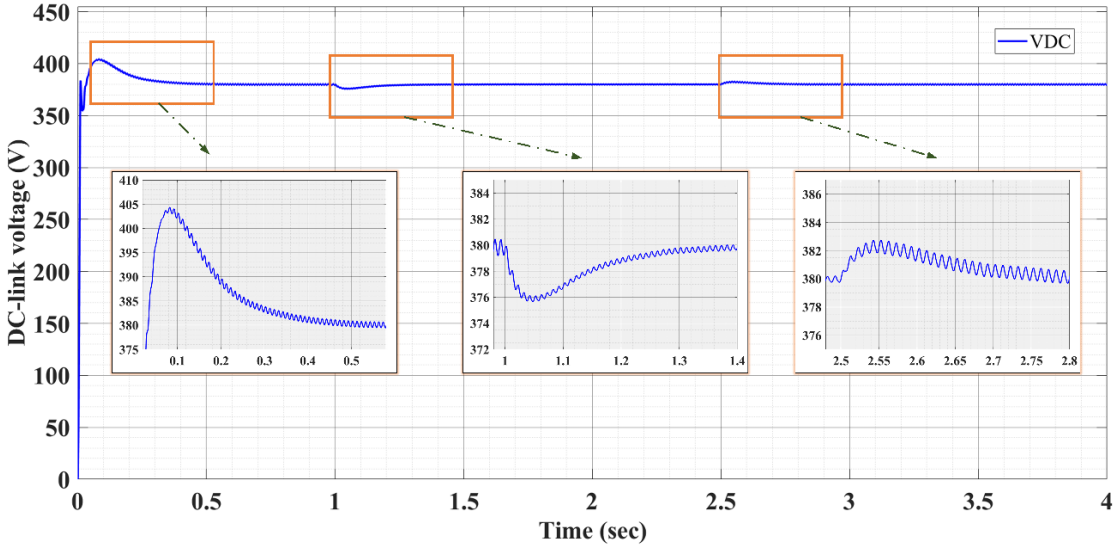

Fig. 9. DC-link voltage

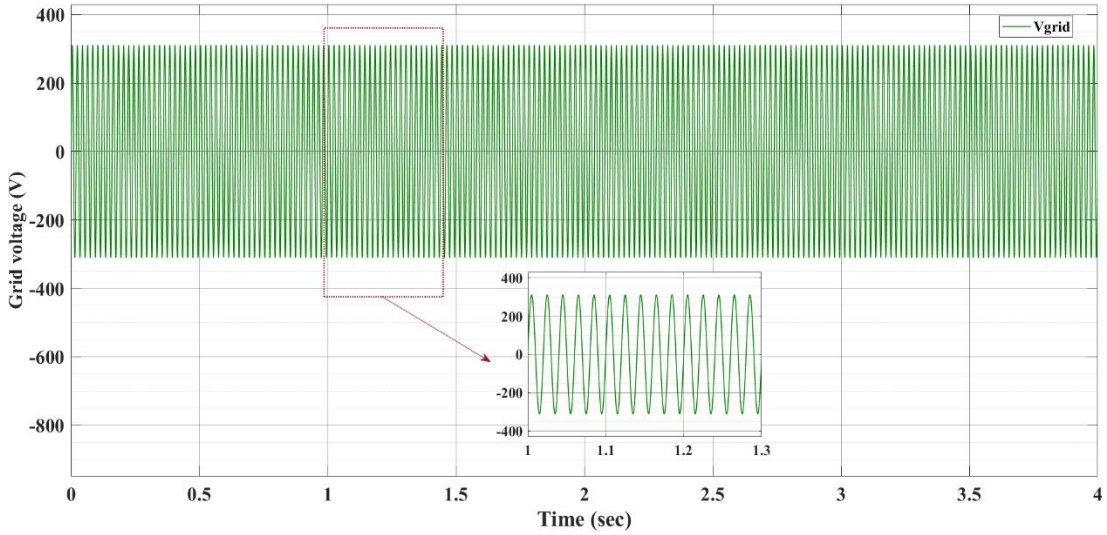

Fig. 10. Grid voltage

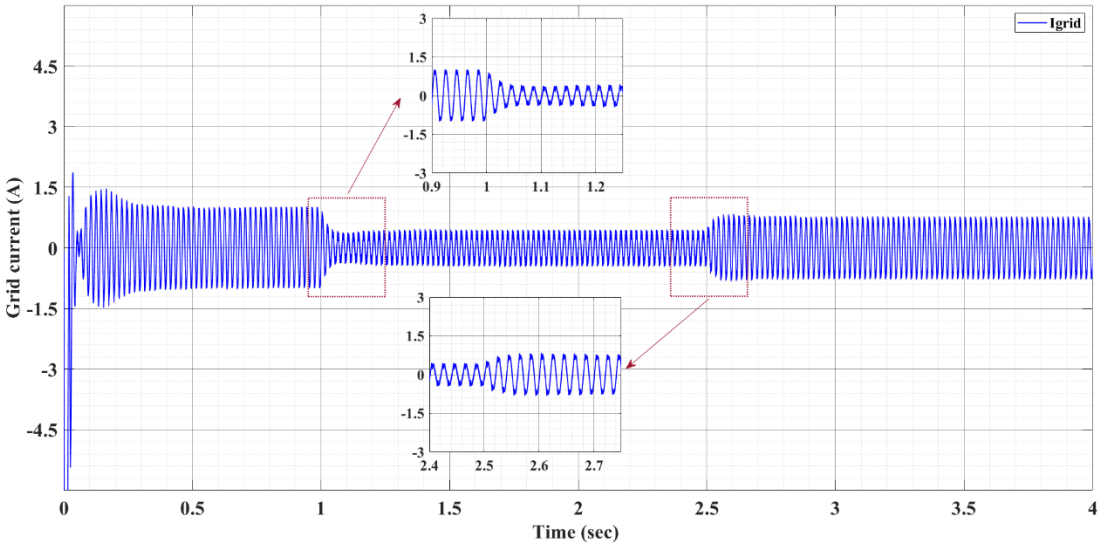

Fig. 11. Grid current

Figure 12 illustrates the MPPT performance graph. As seen in the graph, the MPPT algorithm adapts to the changing irradiance conditions and tracks the PV panel voltage of the V_{ref} value at the MPPT output in a healthy way.

Figure 13 shows a comparison of the adaptive P&Q algorithm. The fixed step size is multiplied by a coefficient determined by the power and voltage variation. It is seen that the MPP tracking performance improves with the adaptive step size obtained in this way.

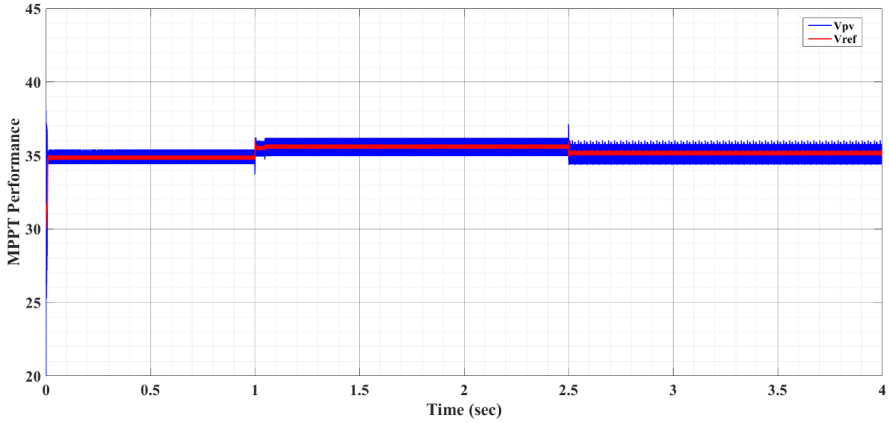

Fig. 12. MPPT performance

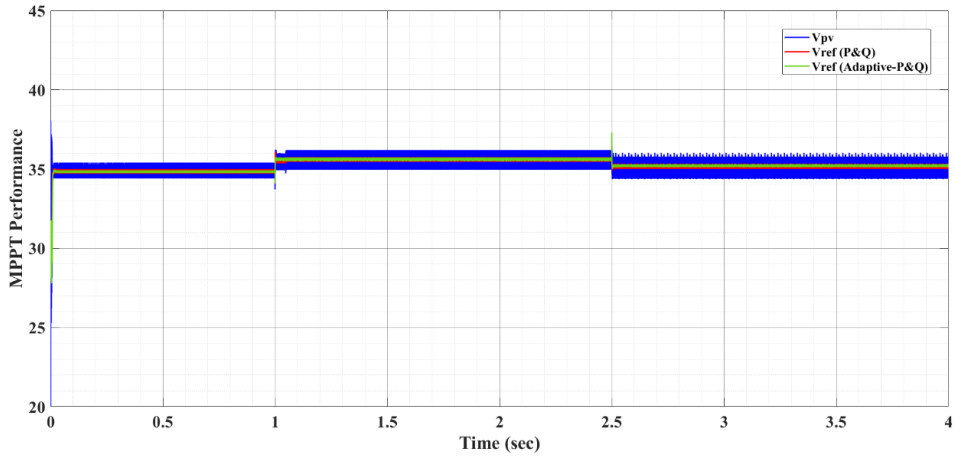

Fig. 13. MPPT performance with Adaptive-P&Q

To evaluate the output current quality of the microinverter, a harmonic analysis is performed using the Fast Fourier Transform (FFT). As shown in Figure 14, the output current exhibits a low level of total harmonic distortion (THD), confirming the effectiveness of the control strategy in ensuring grid compliance.

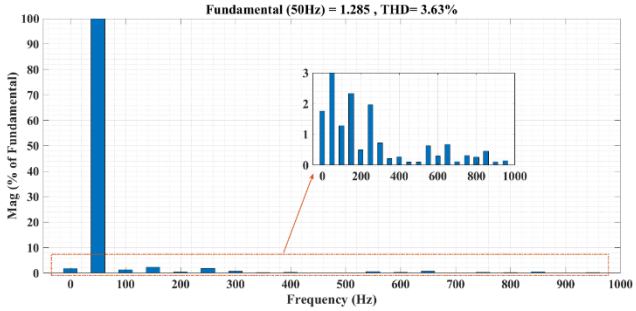

Fig. 14. THD Analysis

VII. Conclusion

This study aims to design a microinverter, which is widely used in photovoltaic systems. The microinverter is designed in MATLAB/Simulink. First, the flyback converter, which is the first stage of the microinverter, is designed. During the design of the converter, the conversion ratio in the transformer is determined by carefully considering the voltage value to be increased. After that, the P&O algorithm and PI control structure are structured for the control of the flyback converter. In the second stage of the microinverter, the DC-AC inverter section and its control structures are formed. Active power control is performed by controlling the DC link voltage with a voltage controller. For the LCL filter, the required calculations are performed, and the grid-connected microinverter design is completed. The design stages are presented in detail. To evaluate the dynamic response of the system, different values of irradiation are applied to the PV panel. In this study, the graphs obtained according to the response of the system at different irradiances indicate that the DC voltage at the output of the flyback converter comes back to 380V. Thanks to the P&Q algorithm and PI controller, the panel voltage and current are at the maximum values that they can produce, and MPP tracking is successfully realized. In the inverter section, DC-AC conversion is performed, and current transfer to the grid is provided by filtering with the designed LCL filter. In different irradiation conditions, the reference current change is determined with the D-Q axis control loop and voltage controller, and the change in the current transferred to the grid is successfully observed

References

[1] C. L. Trujillo, F. Santamaría, and E. E. Gaona, "Modeling and testing of two-stage grid-connected photovoltaic micro-inverters," *Renew. Energy*, vol. 99, pp. 533–542, Dec. 2016.

[2] M. Barghi Latran and A. Teke, "Investigation of multilevel multifunctional grid connected inverter topologies and control strategies used in photovoltaic systems," *Renew. Sustain. Energy Rev.*, vol. 42, pp. 361–376, 2015.

[3] Ö. Çelik, A. Teke, and A. Tan, "Overview of micro-inverters as a challenging technology in photovoltaic applications," *Renew. Sustain. Energy Rev.*, vol. 82, pp. 3191–3206, Feb. 2018.

[4] H. A. Sher and K. E. Addoweesh, "Micro-inverters — Promising solutions in solar photovoltaics," *Energy Sustain. Dev.*, vol. 16, no. 4, pp. 389–400, Dec. 2012.

[5] Ö. Çelik, "Controller design and experimental verification of grid-connected microinverters for photovoltaic applications," Ph.D. dissertation, Dept. Elect. and Electr. Eng., Çukurova Univ., Adana, Turkey, 2019.

[6] L. Hassaine, E. Olias, J. Quintero, and V. Salas, "Overview of power inverter topologies and control structures for grid connected photovoltaic systems," *Renew. Sustain. Energy Rev.*, vol. 30, pp. 796–807, 2014.

[7] R. Hasan, S. Mekhilef, M. Seyedmahmoudian, and B. Horan, "Grid-connected isolated PV microinverters: A review," *Renew. Sustain. Energy Rev.*, vol. 67, pp. 1065–1080, Jan. 2017.

[8] B. Hükümen, "Geniş giriş gerilimi aralıklı solar mikro evirici tasarımı ve uygulaması," M.S. thesis, Dept.Elect. and Electr. Eng., Karabük Univ., Karabük, Turkey, 2024.

[9] R. Hasan and S. Mekhilef, "Highly efficient flyback microinverter for grid-connected rooftop PV system," *Sol. Energy*, vol. 146, pp. 511–522, Apr. 2017.

[10] R. Z. B. R. Umar, "High efficiency photovoltaic grid connected flyback microinverter," Ph.D. dissertation, Institute for Advanced Studies, Malaya Univ., Kuala Lumpur, Malezya, 2023.

[11] F. Ronilaya *et al.*, "A Phase-based Control Method to Control Power Flow of a Grid-connected Solar PV through a Single Phase Micro-inverter," *Int. J. Renew. Energy Res.*, vol. 10, no. v10i2, pp. 912–921, 2020.

[12] M. H. Rezaei and M. Akhbari, "Power decoupling capability with PR controller for Micro-Inverter applications," *Int. J. Electr. Power Energy Syst.*, vol. 136, no. August 2021, p. 107607, Mar. 2022.

[13] E. Kabalcı, "Review on novel single-phase grid-connected solar inverters: Circuits and control methods," *Sol. Energy*, vol. 198, no.

October 2019, pp. 247–274, 2020.
[14] C. Deng, M. Chen, F. Zhang, R. Zheng, and F. Jiang, "A Novel Analog Control Strategy with Simplified Implementation Scheme for Boundary Conduction Mode Flyback Microinverter," *IEEE Trans. Power Electron.*, vol. PP, pp. 1–13, 2025.
[15] C. Haliloğlu, "Şebekeye bağlı fotovoltaik sistemler için araya yerleştirilmiş flyback mikro-evirici tasarımı," M.S. thesis, Dept.Elect. and Electr. Eng., Kahramanmaraş Sütçü İmam Univ., Kahramanmaraş, 2019.
[16] N. Laxmi, V. V. Kumar, and S. T. Sv, "Design and Assessment of DC-DC Interleaved Flyback Stage for Module-Integrated PV Microinverters," *2025 IEEE 1st Int. Conf. Smart Sustain. Dev. Electr. Eng. SSDEE 2025*, pp. 1–6, 2025.
[17] M. Tasnim, A. Sarwar, and F. I. Bakhsh, "Implementation of Flyback DC-DC Converter Topology for DC Power Supply Application," *2025 Int. Conf. Cogn. Comput. Eng. Commun. Sci. Biomed. Heal. Informatics, IC3ECSBHI 2025*, no. 3, pp. 681–686, 2025.
[18] S. Zengin, F. Deveci, and M. Boztepe, "Design of Flyback Micro-inverter for Grid Connected Photovoltaic Systems," *Pamukkale Univ. J. Eng. Sci.*, vol. 21, no. 2, pp. 30–36, 2015.
[19] M. Effendy, K. Hidayat, and H. N. A. Humaidi, "An Interleaved Isolated Flyback Converter with MPPT using Modified P&O Algorithm for Photovoltaic Generators," *Eng. Technol. Appl. Sci. Res.*, vol. 15, no. 3, pp. 22295–22300, 2025.
[20] N. R. B. Soham G. Deshpande, N. R. Bhasme, Soham G. Deshpande, "Modeling and Simulation of Microinverter with Flyback Converter for Grid Connected PV Systems," *Int. J. Electr. Electron. Eng. Res.*, vol. 7, no. 4, pp. 71–82, 2017.
[18] E. Kabalci and A. Boyar, "An Interleaved Flyback Micro Inverter with H5 Topology for Photovoltaic Applications," in *2020 2nd Global Power, Energy and Communication Conference (GPECOM)*, Oct. 2020, pp. 12–17.
[19] J. F. Sultani, "Modelling, design and implementation of D-Q control in single-phase grid-connected inverters for photovoltaic systems used in domestic dwellings," Ph.D. dissertation, Faculty of Technology, De Montfort Univ., Leicester, UK, 2013.
[20] U. Tanrikulu, E. Akboy, and B. Akin, "Design and Analysis of a Flyback Converter With Improved Snubber Cells," *Sigma J. Eng. Nat. Sci.*, vol. 38, no. 4, pp. 2205–2216, 2020.
[21] E. Kabalci and A. Boyar, "Design and Analysis of a Single Phase Flyback Micro Inverter," in *2018 6th International Conference on Control Engineering & Information Technology (CEIT)*, Oct. 2018, pp. 1–6.
[22] E. Baldan and H. Erişti, "Parçalı Gölgelenme Durumunda Yapay Sinir Ağları ve Parçacık Sürü Optimizasyonu Tabanlı Bir Maksimum Güç Noktası Takibi Algoritması," *Kahramanmaraş Sütçü İmam Üniversitesi Mühendislik Bilim. Derg.*, vol. 26, no. 4, pp. 895–908, Dec. 2023.
[23] K. A. El Wahid Hamza, H. Linda, and L. Cherif, "LCL filter design with passive damping for photovoltaic grid connected systems," in *IREC2015 The Sixth International Renewable Energy Congress*, Mar. 2015, pp. 1–4.
[24] A. E. W. H. Kahlane, L. Hassaine, and M. Kherchi, "LCL filter design for photovoltaic grid connected systems," *Third Int. Semin. new Renew. energies*, vol. 8, no. 2, pp. 227–232, 2014.

BIOGRAPHIES

Elif Baldan received her Bachelor's and Master's degrees in the Department of Electrical and Electronic Engineering from Mersin University, Mersin, Turkey, in 2016 and 2019, respectively. She is currently pursuing her Ph.D in Electrical and Electronic Engineering at Mersin University. She works as a Research Assistant at Mersin University. Her research interests include power electronics, renewable energy systems, and power systems.

Özgür Çelik received the M.Sc. and Ph.D. degrees from the Department of Electrical and Electronics Engineering, Çukurova University, Adana, Turkey, in 2015 and 2019, respectively. His research interests include control of power electronic converters, grid integration of renewable energy systems, and energy efficiency applications.

Hüseyin Erişti received the Ph.D. degree in electrical and electronics engineering from Firat University, Türkiye, in 2010. He is currently working as a Professor with the Department of Electrical and Electronics Engineering, Mersin University. His research interests include signal processing, pattern recognition, power quality, power systems, and computer vision.